

AnthroVis: Visual Analysis of 3D Mesh Ensembles for Forensic Anthropology

Submission ID 1041

Abstract

Digital approaches to shape comparison and analysis play a very important role in forensic anthropology. New methods are still emerging and the whole area is experiencing a shift from traditional 2D image data to processing of 3D meshes. Therefore, the visual exploration of 3D meshes and methods for their visual comparison play a crucial role in the anthropological research. In our paper we present a novel AnthroVis tool for visual analysis of 3D mesh ensembles, which was designed in tight cooperation with the domain experts. It aims to enhance their workflow by introducing several visualizations that help to understand the similarities and differences between 3D meshes. AnthroVis in general consists of three methods, which serve as a guidance in the process of the comparison of two or more mesh ensembles. The first method, based on the idea of interactive heat plots, provides an overview of pairwise comparisons in a set of analyzed meshes and enables their filtering and sorting. The second method consists of anthropologically relevant cross-cuts indicating the variability through the set of meshes. The last method uses superimposition principle for pairs of meshes equipped with several visual enhancements indicating local mesh differences in three-dimensional space. The domain expert evaluation was performed primarily on facial images, but the tool proved to be applicable to other areas of forensic anthropology as well. Its usefulness is demonstrated by case studies describing the real situations and problems that are encountered by anthropologists in forensic casework.

Keywords: 3D mesh comparison, heat plot, cross-cut, forensic anthropology

1. Introduction

In the framework of forensic anthropology, experts are presented with a vast range of tasks, spanning from assessing skeletal remains to identifying living persons from photographs or surveillance videos. Advances in 3D technologies, namely those related to recording of spatial images, open new possibilities for multiple areas of forensic anthropological expertise. Generally, by capturing 3D meshes of objects, anthropologists are presented with depth information, which allows a novel insight into recorded visual data. Under proper conditions, e.g., an adequate mesh resolution, high-quality texture, or precise geometry, 3D spatial data have been shown to yield highly accurate and reliable results, admissible even under the scrutiny of various legal systems [1].

One of the largest target domains of the research in the forensic and commercial security sector is the field of facial recognition. A variety of software tools aim to assist with the tasks performed in this field. However, tools applicable for facial image identification in forensic anthropology are mostly fully manual or semi-automatic. In order to quantify the extent of similarity between compared meshes they produce large sets of numerical results. As the amount of data can be overwhelming, it becomes important to design various visualization methods, which can facilitate the decision-making process.

Traditionally, when dealing with 3D meshes, anthropologists are accustomed with visualizing morphological variations by using color maps mapped onto a selected mesh. This representation allows uncovering and localizing dissimilarities between aligned meshes. From the methodological point of view,

however, the color maps suffer from several limitations, which can result in a misleading interpretation. First, anthropologists rely mostly on the rainbow coloring scheme with uneven distribution of colors. This can easily lead to situations where the areas with a small difference are marked with the same color leaving the differences visually unrecognizable. Second, in some cases the edge areas on the 3D meshes may differ quite significantly (see Figure 1). Then the distribution of colors in the color map reflects this highly localized irregularity and the remaining global differences spread across the rest of the model are visually omitted.

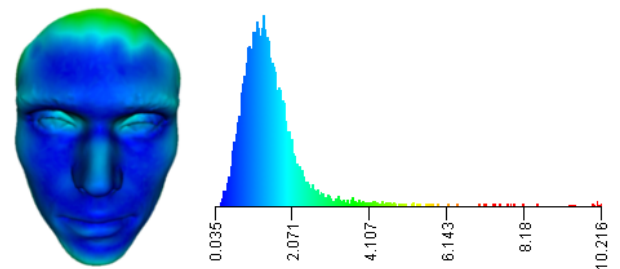


Figure 1: Example of visualization of differences between two meshes using the color map. In case when the boundary areas of the meshes differ significantly (here on the forehead), it leads to uneven distribution of colors. In consequence, the small differences are invisible.

The most straightforward suggestion for improvement would be to remove the parts of the meshes which are significantly different because these often cause the errors on the boundary of the meshes. However, in the case of facial meshes this removal

cannot be performed automatically because some of these differences have significant impact on the comparison. An example of such situation is depicted in Figure 1, where the most different parts of the compared meshes are located close to the boundary but they represent the differences in the height of the forehead. Removing this part will lead to significant and undesirable changes of the input facial model.

In this paper we propose AnthroVis tool for visual analysis of 3D mesh ensembles, which aims to overcome these problems. AnthroVis tool was designed in tight collaboration with the domain experts who also belong to the group of the target users. In the design we emphasized namely the usage of the proposed tool in their workflow. The tool enables the users to compare and match 3D meshes by using an interlinked set of specific visualizations. Most of the visualizations were adopted from other research domains where their usability was already proved. AnthroVis tool was primarily designed for facial meshes but it is equally applicable to other types of meshes. As the evidence of this we provide the real case studies described in the evaluation section. They demonstrate the successful usage of our tool for different tasks performed by the forensic anthropologists – spanning from the identification of persons (e.g., criminals) to the reconstruction of skeletal remains. The identification-related tasks involve mostly the database searching of similar meshes to the reference one. In this process the techniques for comparison of multiple meshes are crucial. When more meshes satisfy the comparison conditions, then more detailed exploration has to be launched. Here methods for the pairwise comparison of the reference mesh with a selected similar mesh are crucial. The most common tasks in skeletal reconstruction are to compare the assembled bones with the original scanned data (when available) or to compare the results of reassembling performed manually and using a modeling tool. These tasks require namely methods for comparison of two meshes.

The paper is organized as follows. Section 2 contains a survey of existing approaches to comparative visualization of meshes and their visual analysis. Section 3 provides the readers with more detailed overview of our proposed tool and its design rationale. This involves also the description of the workflow of the domain experts and points out the main limitations of the current solutions. In Section 4 we introduce our tool, its main features, and design and implementation details of the proposed visualizations. Our results in Section 5 are presented in a form of real case studies which were performed directly by the main experts. In Section 6 we discuss the advantages and current limitations of our solution. Section 7 concludes the paper and outlines the future work.

2. Related Work

Research in the area of mesh comparison is mostly focusing on technical aspects of a given task, such as the distance metrics and comparison algorithms. This section therefore starts with a survey of existing approaches and algorithms for mesh comparison. However, in terms of forensic anthropology, the output of such algorithms needs to be further explored by the experts.

Our tool aims to provide means for such exploration through several interactively linked visualizations. Thus, in the following we focus on the description of the existing approaches related to our proposed visualization methods and visual analysis of mesh or multi-mesh comparison.

2.1. Mesh Comparison

When dealing with 3D data, the comparative algorithms can be divided into two categories: local feature based and holistic algorithms.

Local feature based algorithms are focused on detecting and matching local features, e.g., the approach for facial comparison presented by Gupta et al. based on facial fiducial points [2]. Other feature based algorithms use patches [3, 4] or curves [5] as the bases for comparison.

In case of holistic algorithms, the entire mesh is taken into account. Here belong surface matching algorithms, e.g., Iterative Closest Normal Point method [6], Hausdorff distance based algorithms [7, 8], algorithms based on curvature analysis [9, 10], canonical forms [11], or spherical harmonic features [12].

Some of the existing approaches focus on the comparison of dynamic meshes, such as the algorithm presented by Vasa and Skala [13]. Their approach uses the Hausdorff distance for the comparison. Similarly, also Scharnowski et al. [14] presented their algorithm for comparative visualization of dynamically changing surfaces. Their algorithm, designed mainly for molecular surfaces, uses a deformable model approach to obtain a mapping relation between two surfaces.

2.2. Visual Surface Comparison

When comparing two surfaces, superimposition principle is often used. Transparency plays an important role in this case – a proper level of opacity can improve the understandability of superimposed surfaces purely by modifying the transparency values. In our solution we were inspired by the following techniques which modify the opacity of surfaces based on their geometric properties. Angle-based transparency [15] sets the transparency to the angle between the surface normal and the viewing direction. Born et al. [16] use depth changes and normal variation to detect silhouettes and modify transparency. Another technique, which also adds surface contours to the image, is based on geodesic fragment neighbors search [17].

Other techniques [18, 19, 20] combine superimposition with explicit encoding and introduce features such as curvature strokes and glyphs that indicate the principal curvature directions of surface. Similarly, the distance vectors can connect the corresponding points on two surfaces or indicate other measurements with their size and orientation [21]. Simulation of colorful semitransparent fog filling the space between two surfaces can also show the observer the differences between 3D objects [21].

Among techniques falling into the category of explicit encoding belong techniques based on the color mapping. These methods are often used as the default visualization methods in many applications, including software tools for surface comparison [22, 23], where color is mapped onto the surface of compared 3D meshes.

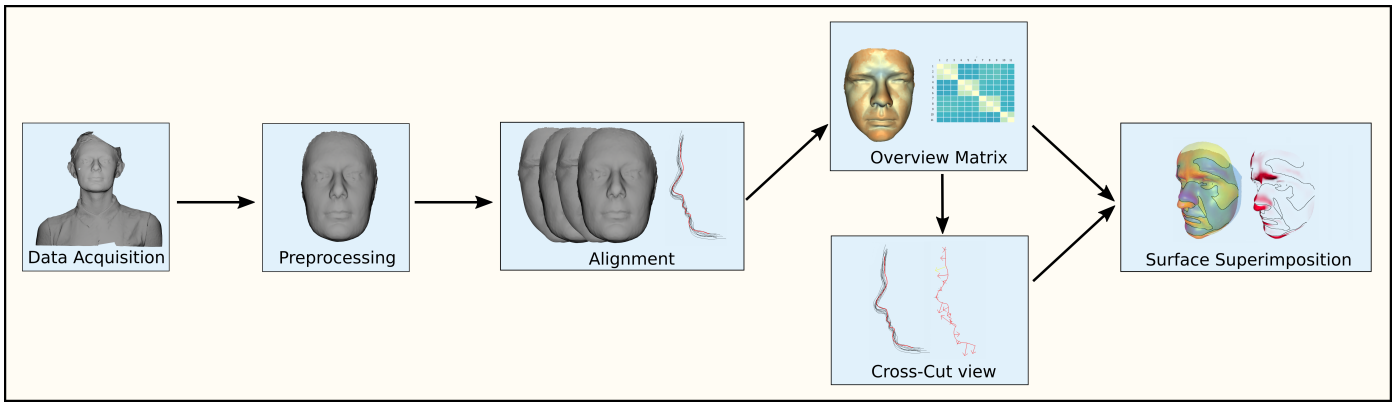


Figure 2: Illustration of the workflow of forensic anthropologists performing the comparison and exploration tasks on a input set of 3D meshes.

155 Zhou and Pang [24] presented a system for comparing sur-¹⁹⁵
 156 face meshes based on different distance metrics and mapped the¹⁹⁶
 157 results onto specific visual representations. The resulting repre-¹⁹⁷
 158 sentations are of varying quality with respect to different levels¹⁹⁸
 159 of detail (reached by the mesh simplification).¹⁹⁹

160 Even with so many visual enhancements at hand, display-²⁰⁰
 161 ing large sets of 3D data at once is ill-advised, due to the high²⁰¹
 162 complexity of images and a lot of visual clutter. A possible so-²⁰²
 163 lution to these problems is the usage of cross-cut views. This²⁰³
 164 approach is widely used in medical visualization for volu-²⁰⁴
 165 metric data – for example CT scan images – where a slice along a²⁰⁵
 166 given plane is projected into 2D space [25]. A similar approach²⁰⁶
 167 is the contouring of specific 3D object features followed by the²⁰⁷
 168 projection of these contours into 2D space. This is often used²⁰⁸
 169 when monitoring the temporal changes of a given feature, e.g.,²⁰⁹
 170 the width of a molecular tunnel [26].²¹⁰

171 Other examples of data simplification by color encoding in-²¹¹
 172 clude heat plots and dense pixel displays [26, 27, 28]. In com-²¹²
 173 bination with interactive options such as thresholding, filtering,²¹³
 174 and data reorganization, they are very effective in discovering²¹⁴
 175 data relationships.²¹⁵

176 2.3. Visual Analysis for Mesh Comparison

177 The techniques mentioned above are usable as standalone²¹⁶
 178 methods for exploration of 3D data. However, when dealing²¹⁷
 179 with large data-sets and wide variety of tasks, such as the ones²¹⁸
 180 posed by the forensic experts, a single view of data is not enough²¹⁹
 181 for thorough analysis.²²⁰

182 Schmidt et al. [23] introduced a toolbox for mesh compari-²²¹
 183 son. Their tool detects hotspots – places with the biggest vari-²²²
 184 ability, and consists of several interconnected visualizations,²²³
 185 such as color maps, lens view, and parallel coordinates view for²²⁴
 186 comparison of meshes at detected hotspots. The tool is limited²²⁵
 187 only to many-to-one mesh comparison scenario.²²⁶

188 Silva et al. [29] published their PolyMeCo tool for com-²²⁷
 189 paring polygonal meshes. This tool focuses on the presenta-²²⁸
 190 tion of the compared meshes but, similarly to the other existing²²⁹
 191 approaches, it uses the color map with the rainbow coloring²³⁰
 192 scheme to convey the differences.²³¹

193 Stalling et al. [30] offered another tool dedicated to visual²³²
 194 data analysis, targeting the general field of life sciences. It sup-²³³

195 ports wide range of tasks, such as image segmentation, geom-¹⁹⁶
 196 etry reconstruction, flow visualizations, or statistical data analy-¹⁹⁷
 197 sis. However, despite its broad scope, it does not address some¹⁹⁸
 198 field specific tasks of forensic anthropology, such as feature de-¹⁹⁹
 199 tection.²⁰⁰

3. AnthroVis Design Rationale

In this section we describe the decisions influencing the design process of the AnthroVis tool and its individual parts. The tool was designed in tight cooperation with the domain experts from forensic anthropology field. To better understand their workflow, we will start with its description. The workflow illustrated in Figure 2 deals with the tasks related to the comparison of two or more 3D meshes. The whole process starts with the data acquisition.

The data are acquired by stereoscopic imaging systems which provide high-poly meshes. In the subsequent preprocessing step the input meshes have to be manually processed because they can suffer from several deficiencies. In case of facial meshes these deficiencies include the parts of the face surrounding, hair, and clothing. These parts are either insignificant to experts or they contain a distorted geometry, which is irrelevant as well. Hence, the final 3D images are trimmed to demarcate the facial area only.

The next step of the workflow performs the alignment and normalization of the meshes. This is done automatically, using the Iterative Closest Point algorithm [31] for minimizing the distance between the input meshes. The alignment represents an important step in the data analysis, as it directly affects its outcome. However, anomalies in the data may cause undesirable distortions of results. As erroneous performance at this stage may lead to failure of the entire analysis, the verification of alignment and normalization results is imperative.

The following stages of the workflow are tightly connected with the comparison and exploration of the meshes. So the tasks performed in these stages directly influence the design of the AnthroVis tool and its visualizations. In the process of facial image identification there are three main commonly performed tasks. The first group of tasks is to explore morphological variations within a set of 3D images in order to quantify the intra-

234 or inter-population variability. The second group deals with²⁸⁸
235 matching an image against a database of images in order to²⁸⁹
236 screen the database and detect similar meshes. Finally, tasks
237 related to matching two images in order to identify or reject the²⁹⁰
238 person's identity form the third group. From these tasks stem²⁹¹
239 the three possible approaches to facial comparison – analyzing²⁹²
240 a set of models (N:N), comparison of one model against a²⁹³
241 dataset (1:N), and comparison of two facial models (1:1).²⁹⁴

242 In 1:1 comparison, a typical goal is to determine whether²⁹⁵
243 two models depict the same person. Here a simple superim-²⁹⁶
244 position of aligned models may provide the idea leading to the²⁹⁷
245 success of this operation. However, such an approach is not²⁹⁸
246 feasible for multiple model comparison.²⁹⁹

247 1:N comparison essentially extends the 1:1 comparison by³⁰⁰
248 matching a primary mesh against a set of secondary meshes. In³⁰¹
249 forensic anthropology this is performed in cases, when multiple³⁰²
250 facial meshes of the same individual should be matched (e.g.,³⁰³
251 in various life stages). The second example can be the case,³⁰⁴
252 when more than one suspect is compared against the evidence³⁰⁵
253 of a perpetrator recorded at a crime scene. Alternatively, two³⁰⁶
254 models are compared and the differences are quantified in order³⁰⁷
255 to specify a causative agent operating in facial differences, e.g.,³⁰⁸
256 age-induced changes, sex-related differences in human face, or³⁰⁹
257 facial variations between relatives.³¹⁰

258 Ultimately, the N:N multiple mesh comparison is based on³¹¹
259 pairwise comparison of models in a dataset. Although in certain³¹²
260 scenarios it also leads to 1:1 comparison, it typically starts with³¹³
261 a different premise. For instance, an exploitation of global and³¹⁴
262 local variability within a sample or a detection of outliers may³¹⁵
263 serve as exemplary cases. As additional data are computed, a³¹⁶
264 simple color map mapped on an average model is not sufficient³¹⁷
265 to visualize such complex results.³¹⁸

266 To support the tasks related to the N:N comparison, An-³¹⁹
267 throVis uses a matrix based visualization providing the users³²⁰
268 with an overview of similarities between all pairs of the input³²¹
269 meshes. By selecting a subset of cells the input set is filtered³²²
270 and the user is navigated to one of the subsequent stages, ac-³²³
271 cording to the content of the selected subset. These stages are³²⁴
272 the cross-cut views serving for 1:N comparison and the surface³²⁵
273 superimposition enabling the 1:1 comparison. In other words,³²⁶
274 through filtering of the data the N:N comparison can lead to the³²⁷
275 1:N and 1:1 comparison stages. The cross-cut visualization al-³²⁸
276 lows the users to observe the local shape and alignment of the³²⁹
277 analyzed meshes using the cutting plane. The surface super-³³⁰
278 imposition is supported by several visual enhancement, such as³³¹
279 transparency or fog simulation, that help users to judge how³³²
280 well the models are aligned. In the following section these pro-³³³
281 posed visualizations will be described in detail.³³⁴

282 4. Visualization Methods³³⁵

283 To support the above mentioned tasks performed by the³³⁶
284 forensic anthropologists, we propose several visualization tech-³³⁹
285 niques and combine them in our unique system for visual anal-³⁴⁰
286 ysis of facial data. Figure 3 shows the overview of the pro-³⁴¹
287 posed visualizations integrated in the AnthroVis tool. The de-³⁴²
288

tails of individual visualization methods were already presented
289 by Furmanova [32].

4.0.1. MatCol – N:N Overview Matrix with Color Map

During the analysis process, a lot of measurements are performed producing many numerical data, particularly in the case of N:N comparison. Displaying them in an understandable way and linking them with the original 3D data is crucial for understanding the similarities and differences between them. Therefore, we propose the MatCol overview matrix, consisting of two parts, the N:N overview matrix (Figure 3d) and the color map with histogram (Figure 3a,b). The MatCol matrix is based on the idea of interactive heat plots and presents the results of pairwise comparison within the input set of all meshes. Each matrix cell represents the value of similarity measurement between two meshes in the dataset. The similarity calculation between these meshes is based on the nearest neighbor matching of the mesh vertices. The acquired distances between the vertices are then statistically processed, depending on the aim of the analysis. For this, one of the following methods can be selected by the user: Root Mean Square, which shows how much values vary from the mean value, 75 Percentile, which thresholds twenty-five percent of the largest distances and only uses maximal value of the thresholded values, thus eliminating possibly erroneous peaks, or Geometric Mean, which determines how values vary from zero, where zero would indicate identical meshes. Other available methods are Minimal Distance and Maximal Distance between the meshes, Variance, and Arithmetic Mean. For each pair of meshes, the result of this calculation is represented by a single number. The N:N overview matrix can be sorted with respect to a selected row or column. It means that the values in the selected row or column are sorted in the ascendant or descendant order and the new order of the cells is projected to the remaining rows or columns as well. This helps to observe trends in the data. To support scalability when analyzing large datasets, we integrated interactive lens tool to the MatCol matrix. The matrix can also serve for subsequent filtering of meshes. Again, the user can select a row or column which leads to 1:N comparison. These selected pairs can be subsequently explored using another proposed visualization, the Cross-cut View. The user can also select one cell of the matrix which corresponds to the selection of a specific pair of meshes. This selection is linked with the Surface Superimposition method dedicated to the comparison of two models (Figure 6). To better perceive the variability in the input dataset, the matrix is also accompanied by histogram showing the distribution of values.

The N:N overview matrix is further extended by the color map view displaying the average mesh computed from the input dataset. This view helps the user to localize the areas with significant differences directly on the mesh. The average mesh is computed in the following way. For each vertex of a user selected reference mesh (one mesh from the analyzed dataset), the nearest neighbor vertices of other meshes are found. Then, a displacement vector is computed from all vectors between the corresponding vertices from the reference mesh and the remaining meshes from the dataset and the reference mesh is modified

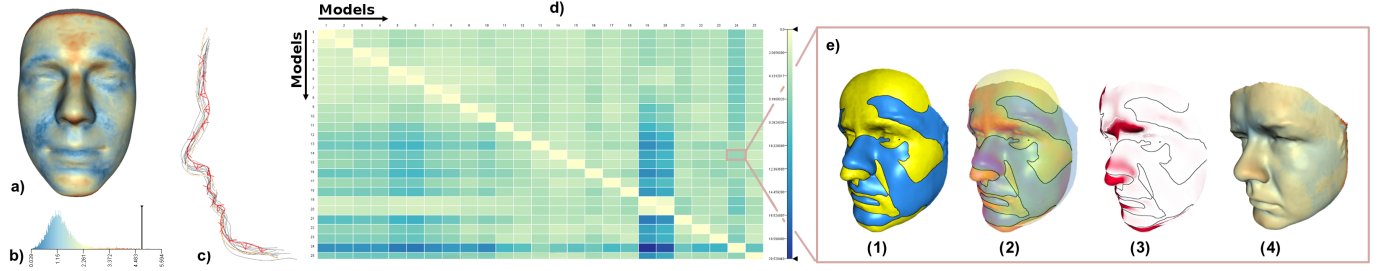


Figure 3: Overview of visualizations integrated in the AnthroVis tool. (a) Color map depicting the average difference between a set of models and the primary model mapped on this primary model. (b) Histogram showing the distribution of values in the used color map. (c) Cross-cut View showing the local shape and alignment of selected meshes using the cutting plane. (d) MatCol overview matrix showing the similarities between pairs of meshes. (e) Surface superimposition views with different enhancements depicting the comparison of the primary model with a selected model from the dataset.

344 by the displacement vectors. This process is repeated iteratively to yield better results and the number of iterations can be defined by the user. The color assigned to each vertex of the average mesh is then computed from the distance to its corresponding vertices in the same way as the values in the N:N overview matrix.

350 4.0.2. CCV – Cross-cut View

351 The MatCol view provides an overview of N:N analysis of models, which is beneficial for the assessment and filtering of the results. However, it does not provide a way to compare the shapes of individual models in the set. For this purpose we propose a cross-cut view (Figure 4).

356 The proposed view was selected because displaying a set of 3D meshes at once is not possible for large datasets, and in any case, it is not very helpful for the shape comparison. In such cases the projection of 3D data into the 2D space is often employed. In our CCV technique we take a slicing plane and compute its intersection with all 3D meshes. The intersections are then displayed in the 2D view. There are three predefined positions of the slicing plane that correspond to the anthropologically relevant contours on the human face. However, as our tool is applicable also to other areas of forensic anthropology, the position and location of the plane can be freely modified by the user. The position of the slicing plane is set and adjustable on a reference mesh visualized in 3D. The reference model can be either the average model of the dataset or a user-selected model.

371 In addition to the intersections with meshes from the dataset the average differences along the intersection with the reference model are computed and displayed. This is done in the following way. The reference intersection curve is uniformly sampled and the normal at each sample point is computed. The difference is then computed as the average distance from the sampling point to the rest of the meshes in the direction of its normal. The shorter the distance vectors the more similar the meshes are at a given point. This visualization is interactively linked with the localized color maps. The selection of a distance vector leads to the selection of the neighborhood of a given point in the color map on the reference model. This allows better understanding of the local variability.

384 Via the selection of secondary intersection contour, the CCV

385 is further linked with our SurfSIM surface superimposition visualization for comparing pairs of meshes in a 1:1 manner. This enables the detailed exploration of differences between the reference and a given target meshes.

389 4.0.3. SurfSIM – Surface Superimposition Method

390 The set of the visualization techniques used for the 1:1 comparison in AnthroVis was adopted from the work of Busking et al. [21]. They proposed a set of techniques for comparison of intersecting surfaces and tested them on medical images. In close cooperation with forensic anthropologists we carefully selected those techniques which can be successfully adopted to their meshes as well.

391 This last set of techniques serves for 1:1 comparison of two selected meshes. The selection of the pair of meshes can be performed in the overview matrix of the MatCol view.

392 The two main demands for this visualization are that it should preserve the shape of both models and clearly indicate the differences between these models. Therefore, we decided to use the superimposition of the aligned meshes supported by the following visual enhancements.

- **Transparency** Transparency modulation can help to solve the problems with occlusion that is one of the most common issues when dealing with 3D models. In our case we split the surfaces of models into two categories with respect to the camera position – the model surface closest to the camera is classified as the *outer surface*, while the surface behind is classified as the *inner surface*. We then keep the inner surface opaque, while making the outer surface transparent. This makes the position of surfaces easier to interpret.
- **Intersection Contours** Highlighting the intersections of models can reveal minor intersections that could be otherwise easily overlooked. The contours are detected on the interfaces between the two meshes where they change their order with respect to the camera position (Figure 3 (e1)).
- **Fog Simulation** This technique simulates a partially transparent volume (fog) filling the space between the two surfaces and assigns it a color different from the colors used for the individual surfaces (Figure 3 (e2,3)). The aim of

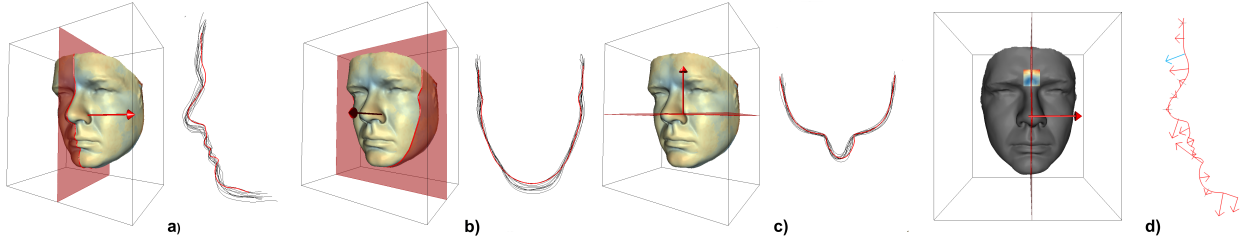


Figure 4: (a,b,c) Three typical facial cuts used by anthropologists. The corresponding cross sections enable to compare contours of ten selected target meshes (black) with the reference mesh (red). (d) Localized color map linked with the variance vectors showing area surrounding the selected vector.

this method is to clearly indicate the differences between the two surfaces. The principle of this method is the following. Lets suppose that the outer surface is nearly completely transparent. In places where the surfaces are close to each other, the thin layer of fog does not occlude the inner surface. However, with the growing distance between surfaces the opacity of the fog accumulates. So in places with larger surface distances the inner surface can be completely covered by the fog. In this case, the distance between the *inner* and *outer* surfaces is computed along the viewing direction. The amount of accumulated fog is proportional to this distance, therefore the whole visualization is view-dependent. In AnthroVis it is also possible to remove the surfaces and show only the fog as an indicator of the volume between these surfaces. By interactive manipulation with the meshes, this method can reveal the local differences that would not be visible in a color map.

As these methods were implemented on GPU, they can be adjusted in real-time and do not require any precomputed results. Therefore, they can easily replace colormaps in places where no precomputed data are available.

represented the primary subject recorded two years prior to the analysis. The ultimate goal was to match the primary subject with its corresponding 3D scan included in the database and at the same time to reject that no other scan could be identified as the primary subject.

In the first step, 10 most similar target faces were selected using the overview matrix visualization. The incorporated ranking function allows sorting the target scans according to the selected measure of similarity, where the most similar meshes are located in the top rows of the overview matrix. This way the user selects n meshes (10 in our case) for further comparisons. For the in-depth analysis, cross-cut visualizations were first employed (see Figure 4). This interactive visualization enables the expert to observe the differences between the scrutinized meshes in cross-section cuts corresponding to three essential anatomical body planes (frontal, sagittal, and transversal) or other optional planes.

Figure 5 (1) shows an example of a comparison between the reference scan and one of the most similar target faces.

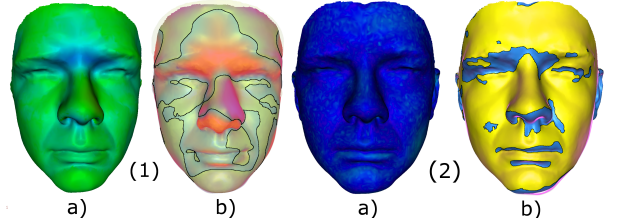


Figure 5: Comparison between two meshes using (a) color map and (b) fog visualization that shows the most significant differences between the input meshes.

For better comparison, the traditionally used color map is also shown. The color map depicts the main differences located in the supraorbital region. However, our proposed visualizations are more successful in demonstrating also other important morphological differences, such as the apparent difference in shape of noses.

As expected, the most similar meshes were those capturing the faces of the specimen in two different time steps (see Figure 5 (2)).

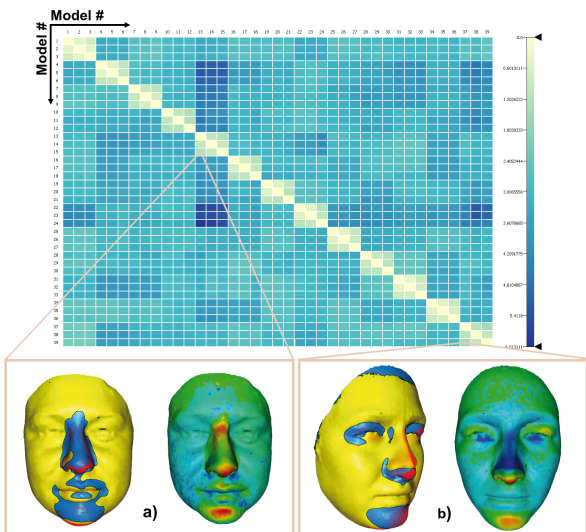
The color map does not reveal noticeable differences because this method is not suitable for revealing minor differences. However, our fog-present superimposition technique shows that although the compared meshes are very similar, they cannot be considered identical. Moreover, the sources of variations can be localized precisely using fog, i.e., in the presented case

501 the tip of the nose, chin, and width of the face.

502 5.2. Case 2 – Facial Identification

503 The second example originates in cases where facial identification is derived from an eyewitness's description of a perpetrator, and frequently combined with the construction of a facial composite. In many cases (e.g., numerous eyewitnesses, distressed indecisive witness), multiple scenarios of a perpetrator's facial appearance have to be confronted. For the present example, 3D scans from 13 individuals were modified in order to explore an impact of these changes on facial identification. Two sets of modifications were created. In the first step, a single facial component (e.g., nose, chin) was modified using a database of 3D facial components. In the next step, additional two components were further switched. Altogether, 39 facial scans were processed using the N:N form of comparison. The results were visualized using the developed MatCol matrix (see Figure 6).

518 It is more that evident that the pairwise comparisons corresponding to the intra-individual scans with the original and 519 modified facial components placed by the plot diagonal exhibit 520 a lower degree of variations than the remaining inter-individual 521 comparisons. The conclusions are supported by the ability to 522 visualize individual compared pairs using either color maps or 523 the additional newly developed techniques.

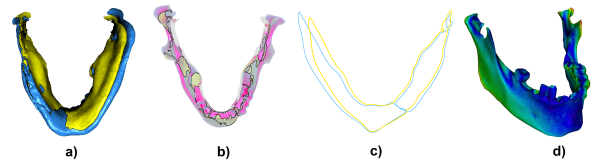


525 Figure 6: Comparison of set of 39 faces of 13 individuals, each present three times with various facial changes. (a) Original mesh compared with mesh with interchanged nose, mouth, and chin. (b) Original mesh compared with mesh with interchanged eyes, nose, and chin.

526 5.3. Case 3 – Fragmentary Skeletal Remains Reassembling

527 The third example focuses on the area of forensic casework, which involves assessment of skeletal remains. In many cases, 528 forensic anthropologists are presented with fractured, fragmented, or otherwise modified human skeletal remains. Prior to anthropological examination, these fragmented remains must be re-assembled. The present case involves a human mandible fractured due to multiple gunshot wounds to the head. The mandibular fragments (presented in three separate pieces) were first laser

534 scanned and the elements were subsequently reassembled in the virtual workspace. Simultaneously, the physical bone fragments were restored in the real physical space by traditional reconstructive approaches. Once reassembled, the physical model was re-digitized in order to confront the virtual and physical approaches. The aim of the study was to reveal the importance of incorporating the virtual approach to the assessment of skeletal injuries. The results are summarized in Figure 7.



535 Figure 7: (a) Comparison between manually (yellow) and virtually (blue) 536 reconstructed mandible from fragmentary skeletal remains. (b) The difference 537 is highlighted using fog. (c) Cross-cut view. (d) Color map.

538 The visual confrontation revealed inconsistencies between the two restoration approaches. The mandible reassembled in the physical reality produced a narrower structure in comparison with the mandible reassembled using the digital fragments. This is particularly apparent from the transparent superimposed meshes with fog highlighting inter-mesh differences.

548 6. Discussion

549 The domain experts confirmed that the AnthroVis tool and 550 its interactive linked visualization techniques can facilitate 551 the everyday decision-making in examining 3D digital evidence 552 in forensic anthropology. The traditional approach utilizing 553 color maps, although considered an advanced visualization tool 554 in forensic and biological sciences (e.g., [1]), has very limited 555 possibilities, particularly while comparing large datasets of 3D 556 facial meshes.

557 The domain experts sorted our visualization techniques by 558 priority in the facial image analysis. The color maps were evaluated 559 as beneficial in cases where the primary goal was to display/evaluate initial basic morphological variations between two 560 faces. Once the initial assessment is performed, however, 561 anthropologists tend to switch to the surface superimposition and 562 the combination of fog and transparent superimposition (in that 563 order), which give a better understanding on minor, local differences 564 between meshes.

565 It also specifies the boundaries of more localized differences. The proper demarcation is particularly important when 566 an expert has to decide whether the observed inconsistencies 567 are due to technical limitations and the two 3D images correspond 568 to the same individual or they represent differences on 569 which the same identity can be undoubtedly rejected.

570 The multiple comparison of faces, previously lacking a suitable 571 technique for the visual exploration, is supported by cross- 572 cuts and the overview matrix. The overview matrix was shown 573 to be extremely helpful when searching for the most similar 574 faces in the dataset or when comparing the specimen with other 575



577 meshes from the dataset. Cross-cuts enable to display local ir-⁶³⁹
 578 regularities in a manner that is rather instinctive for anthropolo-⁶⁴⁰
 579 gists as it is derived from standardized anatomical views and
 580 body planes. Like the anatomical plane, the cross-cuts provide
 581 a common method of communication that helps to avoid con-⁶⁴⁴
 582 fusion when identifying structures and interpreting local differ-⁶⁴⁵
 583 ences.⁶⁴⁶

584 7. Conclusion and Future Work

585 In this paper, we proposed several visualization methods
 586 filling the gaps in the visual exploration of 3D forensic evi-⁶⁵²
 587 dence. Furthermore, we proposed an interactive visual analysis
 588 tool integrating all proposed visualizations, which covers the
 589 current workflow of anthropologists performing these tasks as
 590 much as possible. The tool as well as the visualizations were
 591 tested on real cases and confronted with the currently available
 592 techniques. The testing first aimed to count pros and cons of the
 593 traditional color map approach, and then the newly proposed vi-
 594 sualization techniques were scrutinized accordingly by forensic
 595 anthropologists. The evaluation performed by the domain ex-
 596 perts revealed not only the advantages of the proposed methods
 597 but also their drawbacks, which form possible extensions for
 598 the future work. It was suggested that the fog simulation would
 599 be more beneficial if it was view independent. Finally, con-
 600 cerning the cross sections, it was suggested to add the option of
 601 displaying absolute variability values, as opposed to currently
 602 used relative ones, which take into account the orientation of
 603 vectors.⁶⁷⁴

- [1] Urbanova, P., Hejna, P., Jurda, M.. Testing photogrammetry-based techniques for three-dimensional surface documentation in forensic pathology. *Forensic science international* 2015;250:77–86.
- [2] Gupta, S., Markey, M.K., Bovik, A.C.. Anthropometric 3d face recognition. *International journal of computer vision* 2010;90(3):331–349.
- [3] Guo, Y., Lei, Y., Liu, L., Wang, Y., Bennamoun, M., Sohel, F.. Ei3d: Expression-invariant 3d face recognition based on feature and shape matching. *Pattern Recognition Letters* 2016;.
- [4] Chua, C.S., Han, F., Ho, Y.K.. 3d human face recognition using point signature. In: *Automatic Face and Gesture Recognition*, 2000. Proceedings. Fourth IEEE International Conference on. IEEE; 2000, p. 233–238.
- [5] Bronstein, A.M., Bronstein, M.M., Kimmel, R.. Three-dimensional face recognition. *International Journal of Computer Vision* 2005;64(1):5–30.
- [6] Mohammadzade, H., Hatzinakos, D.. Iterative closest normal point for 3d face recognition. *IEEE transactions on pattern analysis and machine intelligence* 2013;35(2):381–397.
- [7] Huttenlocher, D.P., Klanderman, G.A., Rucklidge, W.J.. Comparing images using the hausdorff distance. *IEEE Transactions on pattern analysis and machine intelligence* 1993;15(9):850–863.
- [8] Pan, G., Wu, Z., Pan, Y.. Automatic 3d face verification from range data. In: *Acoustics, Speech, and Signal Processing*, 2003. Proceedings.(ICASSP'03). 2003 IEEE International Conference on; vol. 3. IEEE; 2003, p. III–193.
- [9] Lei, Y., Li, Q., Song, X., Shi, Z., Chen, D.. 3d face hierarchical recognition based on geometric and curvature features. In: *Computer Network and Multimedia Technology*, 2009. CNMT 2009. International Symposium on. IEEE; 2009, p. 1–4.
- [10] Tanaka, H.T., Ikeda, M., Chiaki, H.. Curvature-based face surface recognition using spherical correlation. principal directions for curved object recognition. In: *Automatic Face and Gesture Recognition*, 1998. Proceedings. Third IEEE International Conference on. IEEE; 1998, p. 372–377.
- [11] Bronstein, A.M., Bronstein, M.M., Kimmel, R.. Expression-invariant representations of faces. *IEEE Transactions on Image Processing* 2007;16(1):188–197.
- [12] Liu, P., Wang, Y., Huang, D., Zhang, Z., Chen, L.. Learning the spherical harmonic features for 3-d face recognition. *IEEE transactions on image processing* 2013;22(3):914–925.
- [13] Vasa, L., Skala, V.. Articulated Motion and Deformable Objects: 4th International Conference, AMDO 2006, Port d'Andratx, Mallorca, Spain, July 11-14, 2006. Proceedings; chap. A Spatio-temporal Metric for Dynamic Mesh Comparison. Berlin, Heidelberg: Springer Berlin Heidelberg. ISBN 978-3-540-36032-2; 2006, p. 29–37.
- [14] Scharnowski, K., Krone, M., Reina, G., Kulschewski, T., Pleiss, J., Ertl, T.. Comparative visualization of molecular surfaces using deformable models. *Computer Graphics Forum* 2014;33(3):191–200.
- [15] Hummel, M., Garth, C., Hamann, B., Hagen, H., Joy, K.I.. IRIS: Illustrative rendering for integral surfaces. *IEEE Transactions on Visualization and Computer Graphics* 2010;16(6):1319–1328.
- [16] Born, S., Wiebel, A., Friedrich, J., Scheuermann, G., Bartz, D.. Illustrative stream surfaces. *IEEE Transactions on Visualization and Computer Graphics* 2010;16(6):1329–1338.
- [17] Carneky, R., Fuchs, R., Mehl, S., Jang, Y., Peikert, R.. Smart transparency for illustrative visualization of complex flow surfaces. *IEEE Transactions on Visualization and Computer Graphics* 2013;19(5):838–851.
- [18] Interrante, V., Fuchs, H., Pizer, S.M., Member, S.. Conveying the 3D shape of smoothly curving transparent surfaces via texture. *IEEE Transactions on Visualization and Computer Graphics* 1997;3:98–117.
- [19] Diewald, U., Preusser, T., Rumpf, M.. Anisotropic diffusion in vector field visualization on Euclidean domains and surfaces. *IEEE Transactions on Visualization and Computer Graphics* 2000;6(2):139–149.
- [20] Weigle, C., Taylor, R.. Visualizing intersecting surfaces with nested-surface techniques. In: *Visualization*, 2005. VIS 05. IEEE. 2005, p. 503–510.
- [21] Busking, S., Botha, C.P., Ferrarini, L., Milles, J., Post, F.H.. Image-based rendering of intersecting surfaces for dynamic comparative visualization. *The Visual Computer* 2011;27: 347–363.
- [22] EDF R&D, T.P.. CloudCompare (version 2.9) [GPL software]. 2017. Retrieved from <http://www.cloudcompare.org/>.
- [23] Schmidt, J., Preiner, R., Auzinger, T., Wimmer, M., Groeller, M., Bruckner, S.. YMCA – your mesh comparison application. In: *Visual Analytics Science and Technology (VAST)*, 2014 IEEE Conference on. 2014, p. 153–162.
- [24] Zhou, L., Pang, A.. Metrics and visualization tools for surface mesh comparison. In: *Photonics West 2001-Electronic Imaging*. International Society for Optics and Photonics; 2001, p. 99–110.
- [25] Fries, K.I., Blanke, P., Wolter, F.E.. YaDiV - an open platform for 3D visualization and 3D segmentation of medical data. *The Visual Computer* 2011;27(2):129–139.
- [26] Byska, J., Jurcik, A., Groeller, M.E., Viola, I., Kozlikova, B.. MoleCollar and Tunnel Heat Map visualizations for conveying spatio-temporal chemical properties across and along protein voids. *Computer Graphics Forum* 2015;3(34):1–10.
- [27] Ivanisevic, J., Benton, H.P., Rinehart, D., Epstein, A., Kurczy, M.E., Boska, M.D., et al. An interactive cluster heat map to visualize and explore multidimensional metabolomic data. *Metabolomics* 2014;1:1–6.
- [28] Zhai, Y., Huang, X., Chang, X.. Combining least absolute shrinkage and selection operator (LASSO) and heat map visualization for biomarkers detection of LGL leukemia. In: *Systems and Information Engineering Design Symposium (SIEDS)*, 2015. 2015, p. 165–170.
- [29] Silva, S., Madeira, J., Santos, B.S.. PolyMeCo – a polygonal mesh comparison tool. In: *Information Visualisation*, 2005. Proceedings. Ninth International Conference on. 2005, p. 842–847.
- [30] Stalling, D., Westerhoff, M., Hege, H.C.. 38-amira: a highly interactive system for visual data analysis. *Visualization Handbook* 2005;.
- [31] Besl, P.J., McKay, N.D.. Method for registration of 3-D shapes. In: *Robotics-DL tentative*. International Society for Optics and Photonics; 1992, p. 586–606.
- [32] Furmanova, K.. Visualization techniques for 3d facial comparison. In: *Proceedings of the International Summer School on Visual Computing*. ISBN 978-3-8396-0960-6; 2015, p. 23–33.
- [33] Kotulanova, Z., Chalas, I., Urbanova, P.. 3D Virtual Model Database of Human Faces: Applications in anthropology and forensic sciences. In: *Mikulov Anthropology Meeting*. The Dolni Vestonice Studies 20. Brno; 2014, p. 177–180.